# Planar Cable-Direct-Driven Robots, Part I: Kinematics and Statics

**Robert L. Williams II**
Ohio University
Athens, Ohio

**Paolo Gallina**
University of Padova
Padova, Italy

DETC2001/DAC-21145
Proceedings of the
**2001 ASME Design Technical Conferences**
**27th Design Automation Conference**
September 9-12, 2001, Pittsburgh, PA

Contact information:

**Robert L. Williams II**
Associate Professor
Department of Mechanical Engineering
257 Stocker Center
Ohio University
Athens, OH 45701-2979
Phone: (740) 593-1096
Fax: (740) 593-0476
E-mail: williar4@ohio.edu
URL: http://www.ent.ohiou.edu/~bobw

**Proceedings of DETC2001**
**2001 ASME Design Engineering Technical Conferences**
**September 9-12, 2001, Pittsburgh, PA**

# DETC2001/DAC-21145

## PLANAR CABLE-DIRECT-DRIVEN ROBOTS, PART I: KINEMATICS AND STATICS

**Robert L. Williams II**
Ohio University
Athens, OH

**Paolo Gallina**
University of Padova
Padova, ITALY

### ABSTRACT

A hybrid parallel/serial manipulator architecture is introduced where the translational freedoms are provided by a cable-direct-driven robot (CDDR) and the rotational freedoms are provided by a serial wrist mechanism. The motivation behind this work is to improve the serious cable interference problem with existing CDDRs and to avoid configurations where negative cable tensions are required to exert general forces on the environment. Only the translational CDDR is considered in this paper; including kinematics and statics modeling, and determination of the statics workspace (the space wherein all possible Cartesian forces may be exerted with only positive cable tensions). Examples are presented to compare the planar 3-cable CDDR with one degree of actuation redundancy and the 4-cable CDDR with two degrees of actuation redundancy. It was found that the 4-cable case requires less cable tensions and thus less energy compared to the 3-cable case in performing the same simulated tasks.

### 1. INTRODUCTION

Cable-direct-driven robots (CDDRs) are a type of parallel manipulator wherein the end-effector link is supported in-parallel by $n$ cables with $n$ tensioning motors. In addition to the well-known advantages of parallel robots relative to serial robots, CDDRs also have very low mass and even better stiffness than other parallel robots. Several CDDRs and cable-direct-driven haptic interfaces (CDDHIs) have been studied in the past. An early CDDR is the *Robocrane* developed by NIST for use in shipping ports (Albus, et. al., 1993). This device is similar to an upside-down six-degrees-of-freedom (dof) Stewart platform, with six cables instead of hydraulic-cylinder legs. In this system, gravity is an implicit actuator that ensures cable tension is maintained at all times. Another CDDR is *Charlotte*, developed by McDonnell-Douglas (Campbell, et. al., 1992) for use on International Space Station. *Charlotte* is a rectangular box driven in-parallel by eight cables, with eight tensioning motors mounted on-board (one on each corner). Four CDDHIs have been built and tested, the *Texas 9-string* (Lindemann and Tesar, 1989), the *SPIDAR* (Ishii and Sato, 1994), the 7-cable master (Kawamura and Ito, 1993), and the 8-cable haptic interface (Williams, 1998). CDDRs and CDDHIs can be made lighter, stiffer, safer, and more economical than traditional serial robots and haptic interfaces since their primary structure consists of lightweight, high load-bearing cables. On the other hand, one major disadvantage is that cables can only exert tension and cannot push on the moving platform.

All of the devices discussed above are designed with actuation redundancy, i.e. more cables than wrench-exerting degrees-of-freedom (except for the *Robocrane*, where tensioning is provided by gravity) in attempt to avoid configurations where certain wrenches require an impossible compression force in one or more cables. Despite actuation redundancy, there exist subspaces in the potential workspace where some cables can lose tension. Roberts et al. (1998) developed an algorithm for CDDRs to predict if all cables are under tension in a given configuration while supporting the robot weight only. The current authors have developed best CDDHI design with regard to wrenches with only positive cable tensions and with regard to avoiding cable interference (Williams and Gallina, 2000). It was found that cable interference dominates.

Most proposed CDDRs and CDDHIs involve both translational and rotational motion of the end-effector link guided by cables. (The single exception is the *SPIDAR* by Ishii and Sato (1994) which is a spatial 4-cable haptic interface reading translations only and providing three Cartesian forces to the human finger.) All CDDRs and CDDHIs with translational and rotational motion suffer from the potential of cable interference and reduced statics workspaces wherein some negative cable tensions would be required, which is infeasible. The basic idea behind this paper is to introduce a new hybrid manipulator and haptic interface structure wherein the translational motion and forces are provided by cables and the rotational motion and moments by a serial wrist mechanism. Hybrid serial/parallel manipulators have been proposed (an early reference is Sklar and Tesar, 1988). To the authors' knowledge, this concept has not been previously extended to CDDRs. Also, Sklar and Tesar (1988) and many serial/parallel manipulators proposed since consist of serial manipulators with parallel joints. The current concept is a parallel CDDR with a serial wrist mechanism mounted at the end-point. The main objective of this work is to benefit from potential

advantages of CDDRs without the cable interference and negative cable tension problems.

This paper describes two candidate planar CDDRs, presents kinematics modeling, followed by statics modeling, a method for attempting to maintain positive cable tensions, and then examples for planar CDDRs with one and two degrees actuation redundancy. This paper focuses only on the translational motion and forces via cables.

## 2. CABLE-DIRECT-DRIVEN ROBOTS (CDDRs)

In this paper a CDDR consists of a single end-effector point supported in parallel by *n* cables controlled by *n* tensioning actuators. Figures 1 and 2 show the planar 3-cable and 4-cable CDDR kinematics diagrams. We are introducing the concept of hybrid CDDRs, where the translational freedoms are provided by the *n* cables and the rotational freedoms can be provided by a serial wrist mechanism. We are considering only the translational portion of the problem here.

For 2-dof planar translations there must be at least two cables. Since cables can only exert tension on the end-effector, there must be more cables to avoid configurations where the robot can be slack and lose control. Figure 1 represents one degree of actuation redundancy, i.e. three cables to achieve the two Cartesian degrees-of-freedom $\mathbf{X} = \{x \quad y\}^T$; the CDDR in Fig. 2 has two degrees of actuation redundancy. These scenarios represent actuation redundancy but not kinematic redundancy. That is, there are extra motor(s) which provides infinite choices for applying 2-dof Cartesian force vectors, but the moving point has only two Cartesian degrees-of-freedom ($\mathbf{X} = \{x \quad y\}^T$, the components of the vector from the origin of {**0**} to the moving point, expressed in {**0**}). Figures 1 and 2 show the reference frame {**0**} whose origin is the centroid of the base polygon; the regular base polygon (triangle and square, respectively) has sides of fixed length $L_B$; each cable is attached to the ground link at $\mathbf{A}_i = \{A_{ix} \quad A_{iy}\}^T$; the length of each cable is denoted as $L_i$, and the cable angles are $\theta_i$ ($i = 1,2,\cdots,n$).

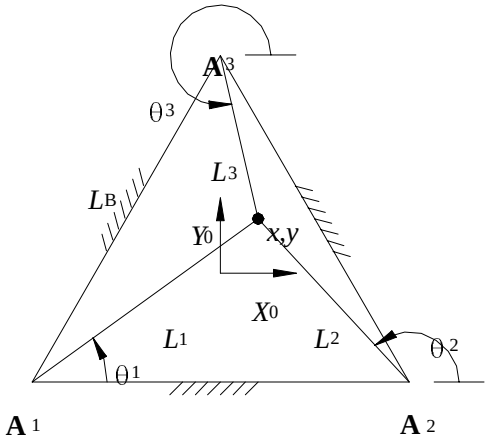


*Figure 1. Planar 3-Cable CDDR Kinematics Diagram*

Theoretically the moving point can reach any point within the base polygon, if cable lengths can go to zero. Also, the potential for cable/cable and cable/end-point interference is non-existent for the CDDR designs of Figs. 1 and 2. The potential certainly exists for interference between cables and workspace items and/or humans, but this problem can be minimized by design in the case of planar CDDRs.

## 3. CDDR KINEMATICS MODELING

This section presents the inverse and forward translational position and velocity kinematics analysis for planar CDDRs. Inverse kinematics is required for control, and forward kinematics is required for simulation and sensor-based control. Position kinematics is concerned with relating the active joint variables and rates to the Cartesian position and rate variables of the moving point. The cable angles and rates are also involved. Assuming all cables always remain in tension, CDDR kinematics is similar to in-parallel-actuated robot kinematics (e.g. Tsai, 1999; Gosselin, 1996); however, with CDDRs the joint space is overconstrained with respect to the Cartesian space.

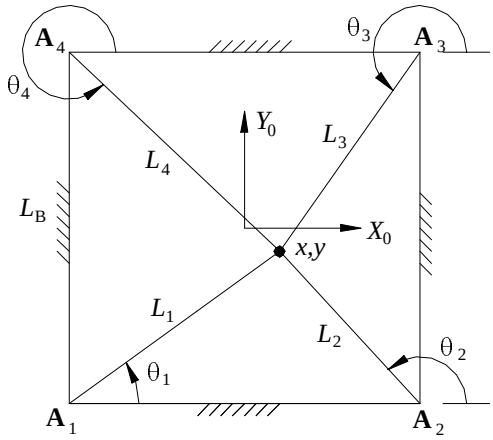


*Figure 2. Planar 4-Cable CDDR Kinematics Diagram*

### 3.1 Position Kinematics

The inverse position kinematics problem is stated: given the Cartesian position $\mathbf{X} = \{x \quad y\}^T$ calculate the cable lengths $L_i$. The solution is simply calculating the Euclidean norm between the moving point $\mathbf{X} = \{x \quad y\}^T$ and each fixed ground link vertex $\mathbf{A}_i$:

$$L_i = \sqrt{(x - A_{ix})^2 + (y - A_{iy})^2} \qquad i = 1,\cdots,n \qquad (1)$$

For use in velocity kinematics and statics, we require the cable angles:

$$\theta_i = \tan^{-1}\left(\frac{y - A_{iy}}{x - A_{ix}}\right) \qquad i = 1,\cdots,n \qquad (2)$$

The quadrant-specific inverse tangent function should be used in (2).

The forward position kinematics problem is stated: given the cable lengths $L_i$, calculate the Cartesian position $\mathbf{X} = \{x \quad y\}^T$. This problem is overconstrained and assumes a consistent input of $L_i$. First we consider cables 1 and 2. This problem can be simplified by shifting a new reference frame origin to $\mathbf{A}_1$ whose *XY*

directions are identical to {**0**}; in this new frame $\mathbf{A}_1 = \{0 \quad 0\}^T$ and $\mathbf{A}_2 = \{L_B \quad 0\}^T$. Then the solution to the forward position kinematics problem is the intersection of two circles, one centered at $\mathbf{A}_1$ with radius $L_1$ and the second centered at $\mathbf{A}_2$ with radius $L_2$; the result is:

$$x = \frac{L_B^2 + L_1^2 - L_2^2}{2L_B} \qquad y = \pm\sqrt{L_1^2 - x^2} \tag{3}$$

We choose the positive solution for *y* in (3) to ensure the forward position kinematics solution lies within the ground polygon. Therefore, from the multiple possibilities (we could have used any two cables to obtain the solution), there is a unique correct solution. Note the value of *x* in (3) is unique due to the special geometry for cables 1 and 2 (both *y* values have the same *x* value). To finish, this solution (3) must be shifted back to the {**0**} frame reference. This solution applies to any planar *n*-cable CDDR.

After employing (3) for the forward position kinematics solution, it is a good idea to use the inverse position kinematics solution (1) for all remaining cables ( $i = 3, \cdots, n$ ) to verify that the $L_i$ input was consistent.

### 3.2 Velocity Kinematics

To derive the velocity kinematics equations we consider the $i^{th}$ cable vector-loop-closure equation $\{x \quad y\}^T = \{A_{ix} + L_i c\theta_i \quad A_{iy} + L_i s\theta_i\}^T$, where $c\theta_i = \cos(\theta_i)$ and $s\theta_i = \sin(\theta_i)$. The time derivative yields:

$$\begin{Bmatrix} \dot{x} \\ \dot{y} \end{Bmatrix} = \begin{bmatrix} c\theta_i & -L_i s\theta_i \\ s\theta_i & L_i c\theta_i \end{bmatrix} \begin{Bmatrix} \dot{L}_i \\ \dot{\theta}_i \end{Bmatrix} \qquad i = 1, \cdots, n \tag{4}$$

We invert this $i^{th}$ cable Jacobian matrix to yield:

$$\begin{Bmatrix} \dot{L}_i \\ \dot{\theta}_i \end{Bmatrix} = \begin{bmatrix} c\theta_i & s\theta_i \\ -s\theta_i / L_i & c\theta_i / L_i \end{bmatrix} \begin{Bmatrix} \dot{x} \\ \dot{y} \end{Bmatrix} \qquad i = 1, \cdots, n \tag{5}$$

Since we are interested in relating active cable length rates to the Cartesian rates, we can extract the first row of (5) to construct the overall CDDR inverse velocity solution. For the 3- and 4-cable cases:

$$\begin{Bmatrix} \dot{L}_1 \\ \dot{L}_2 \\ \dot{L}_3 \end{Bmatrix} = \begin{bmatrix} c\theta_1 & s\theta_1 \\ c\theta_2 & s\theta_2 \\ c\theta_3 & s\theta_3 \end{bmatrix} \begin{Bmatrix} \dot{x} \\ \dot{y} \end{Bmatrix} \qquad \begin{Bmatrix} \dot{L}_1 \\ \dot{L}_2 \\ \dot{L}_3 \\ \dot{L}_4 \end{Bmatrix} = \begin{bmatrix} c\theta_1 & s\theta_1 \\ c\theta_2 & s\theta_2 \\ c\theta_3 & s\theta_3 \\ c\theta_4 & s\theta_4 \end{bmatrix} \begin{Bmatrix} \dot{x} \\ \dot{y} \end{Bmatrix} \tag{6}$$

Note that though we eliminated $\dot{\theta}_i$ from the velocity equations, cable angles $\theta_i$ from (2) are required in (6). The general form of (6) is $\dot{\mathbf{L}} = \mathbf{M}\dot{\mathbf{X}}$ where $\dot{\mathbf{L}}$ is the vector of *n* cable rates, $\mathbf{M}$ is the CDDR inverse Jacobian matrix, and $\dot{\mathbf{X}} = \{\dot{x} \quad \dot{y}\}^T$ is the Cartesian velocity vector for the moving point, shared by all *n* cables. Considering the inverse velocity problem of conventional serial robots, the result (6) is amazing: the inverse velocity problem is solved directly (the inversion was handled symbolically from (4) to (5)) with little computation and there is no singularity problem.

However, to solve the forward velocity kinematics problem we must invert the form of (6): $\dot{\mathbf{X}} = \mathbf{M}^{-1}\dot{\mathbf{L}}$. Due to redundant actuation, $\mathbf{M}$ is not square but is of dimension *n*x2 for the planar case; therefore we cannot invert $\mathbf{M}$ but we have two choices for the forward velocity solution: 1) choose only two cables to make a reduced, square, inverse Jacobian matrix. For instance, as in the forward position kinematics solution, choose cables 1 and 2. The forward velocity solution for the 3-cable CDDR is then $\dot{\mathbf{X}} = \mathbf{M}_{12}{}^{-1}\dot{\mathbf{L}}_{12}$ where $\mathbf{M}_{12}$ is $\mathbf{M}$ with row 3 removed and $\dot{\mathbf{L}}_{12}$ is the vector containing the first two cable rates. This approach can readily be extended to the 4-cabe CDDR. After forward velocity solution, ensure that the $\dot{\mathbf{L}}$ inputs were consistent by evaluating the neglected row(s) of (6). 2) The alternate forward velocity solution approach, assuming consistent $\dot{\mathbf{L}}$ inputs, is to use the overconstrained Moore-Penrose pseudoinverse: $\dot{\mathbf{X}} = \mathbf{M}^{\#}\dot{\mathbf{L}}$, where $\mathbf{M}^{\#} = \left(\mathbf{M}^{\mathbf{T}}\mathbf{M}\right)^{-1}\mathbf{M}^{\mathbf{T}}$.

Via either solution approach, the forward velocity solution is subject to singularities. The singularity conditions are derived from the determinants of the three possible 2x2 square submatrices of $\mathbf{M}$:

$$\begin{aligned} \sin(\theta_2 - \theta_1) = 0 \qquad & \theta_2 - \theta_1 = 0, \pi, \cdots \\ \sin(\theta_3 - \theta_2) = 0 \qquad & \theta_3 - \theta_2 = 0, \pi, \cdots \\ \sin(\theta_1 - \theta_3) = 0 \qquad & \theta_1 - \theta_3 = 0, \pi, \cdots \end{aligned} \tag{7}$$

The singularities only occur when two cables lie along a straight line; this is only possible at the edges of the theoretical kinematic workspace, i.e. along the edges of the ground polygon. Equation (7) gives the 3-cable CDDR singularities. The 4-cable CDDR singularities are similar.

## 4. CDDR STATICS MODELING

In this paper, the workspace wherein all cables are under positive tension while exerting all possible Cartesian forces is called the statics workspace. Statics modeling and attempting to maintain positive cable tension are presented in this section. We use a simple method to determine the extent of the statics workspace, i.e. the workspace wherein all possible forces can be applied with positive cable tensions.

### 4.1 Statics Modeling

This section presents statics modeling for planar CDDRs. For static equilibrium the sum of forces exerted on the moving point by the cables must equal the resultant external force exerted on the environment. Figure 3 shows the statics free-body diagram for the planar 4-cable CDDR.

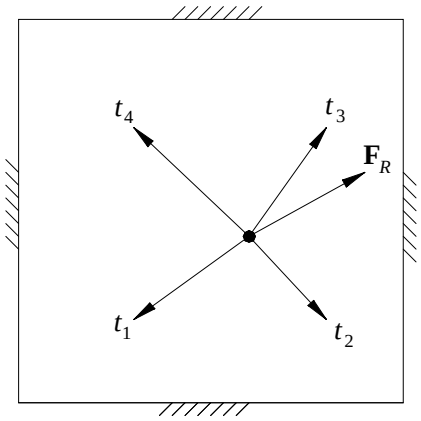


*Figure 3. Planar 4-Cable CDDR Statics Diagram*

The statics equations are:

$$\sum_{i=1}^{n} \underline{t}_i = -\sum_{i=1}^{n} t_i \hat{\mathbf{L}}_i = \mathbf{F}_R \tag{8}$$

In this paper gravity is ignored because it is assumed to be perpendicular to the CDDR plane; we assume the moving point is supported on a plane. All vectors are expressed in $\{\mathbf{0}\}$ (see Figs. 1 and 2). In (8), $t_i$ is the cable tension applied to the $i^{th}$ cable (opposite the cable length unit direction $\hat{\mathbf{L}}_i = \{c\theta_i \quad s\theta_i\}^T$ because $\mathbf{t}_i$ must be in tension). $\mathbf{F}_R = \{f_x \quad f_y\}^T$ is the resultant vector force exerted on the environment by the moving point. Substituting terms into (8) yields the form $\mathbf{ST} = \mathbf{F}_R$, where $\mathbf{S} = \left[-\hat{\mathbf{L}}_1 \quad \cdots \quad -\hat{\mathbf{L}}_n\right]$ is the 2x*n* Statics Jacobian matrix and $\mathbf{T} = \{t_1 \quad \cdots \quad t_n\}^T$ is the vector of scalar cable tensions $t_i$. For the 3- and 4-cable CDDRs:

$$\begin{bmatrix} -c\theta_1 & -c\theta_2 & -c\theta_3 \\ -s\theta_1 & -s\theta_2 & -s\theta_3 \end{bmatrix} \begin{Bmatrix} t_1 \\ t_2 \\ t_3 \end{Bmatrix} = \begin{Bmatrix} f_x \\ f_y \end{Bmatrix} \tag{9a}$$

$$\begin{bmatrix} -c\theta_1 & -c\theta_2 & -c\theta_3 & -c\theta_4 \\ -s\theta_1 & -s\theta_2 & -s\theta_3 & -s\theta_4 \end{bmatrix} \begin{Bmatrix} t_1 \\ t_2 \\ t_3 \\ t_4 \end{Bmatrix} = \begin{Bmatrix} f_x \\ f_y \end{Bmatrix} \tag{9b}$$

Note that there is a special duality between force and inverse velocity: these respective Jacobian matrices are related by $\mathbf{S} = -\mathbf{M}^T$; compare (6) and (9). The statics equations (9) can be inverted in an attempt to exert general Cartesian forces while maintaining positive cable tension. This work is presented in the next subsection.

### 4.2 Maintaining Positive Cable Tension

For CDDRs with actuation redundancy, (9) is underconstrained which means that there are infinite solutions to the cable tension vector $\mathbf{T}$ to exert the given Cartesian force $\mathbf{F}_R$. To invert (9) (solving the required cable tensions $\mathbf{T}$ given the desired force $\mathbf{F}_R$) we adapt the well-known particular and homogeneous solution from rate control of kinematically-redundant serial manipulators:

$$\mathbf{T} = \mathbf{S}^+ \mathbf{F}_R + \left(\mathbf{I}_n - \mathbf{S}^+ \mathbf{S}\right)\mathbf{z} \tag{10}$$

where $\mathbf{I}_n$ is the *n*x*n* identity matrix, $\mathbf{z}$ is an arbitrary *n*-vector, and $\mathbf{S}^+ = \mathbf{S}^T\left(\mathbf{S}\mathbf{S}^T\right)^{-1}$ is the *n*x2 underconstrained Moore-Penrose pseudoinverse of $\mathbf{S}$. The first term of (10) is the particular solution to achieve the desired force, and the second term is the homogeneous solution that maps $\mathbf{z}$ to the null space of $\mathbf{S}$.

***4.2.1 One Degree of Actuation Redundancy.*** For CDDRs with only one degree of actuation redundancy (the planar 3-cable case in this paper), the positive cable tension method of Shen et al. (1994) is adapted to determine the extent of the statics workspace. For actuation redundancy of degree one, an equivalent expression for (10) is:

$$\mathbf{T} = \begin{Bmatrix} t_{P1} \\ t_{P2} \\ t_{P3} \end{Bmatrix} + \alpha \begin{Bmatrix} n_1 \\ n_2 \\ n_3 \end{Bmatrix} \tag{11}$$

where the particular solution $\mathbf{S}^+\mathbf{F}_R$ is the first term in (11) and the homogeneous solution is expressed as the kernel vector of $\mathbf{S}$ ($\mathbf{N} = \{n_1 \quad n_2 \quad n_3\}^T$) multiplied by arbitrary scalar $\alpha$.

The method we adapt from Shen et al. (1994) to determine if a given point lies within the statics workspace for a given CDDR is simple. To ensure positive tensions $t_i$ on all cables *i* = 1,2,3, *for all possible exerted forces*, it is necessary and sufficient that all kernel vector components ($n_i$, *i* = 1,2,3) have the same sign. That is, for a given point to lie within the statics workspace, all $n_i > 0$ OR all $n_i < 0$ (*i* = 1,2,3). If one of these two conditions is satisfied, regardless of the particular solution, we can find a scalar $\alpha$ in (11) which guarantees that all cable tensions $\mathbf{T}$ are positive by adding (or subtracting) enough homogeneous solution. Note a strict inequality is required; if one or more $n_i = 0$, the point in question does not lie within the statics workspace. This method is simple but powerful since we needn't consider specific forces, but it works for *all possible forces*. It should also be noted that while we demonstrate this method for the planar 3-cable CDDR, it is applicable to any planar and spatial CDDR with one degree of actuation redundancy.

The method to calculate each kernel vector component is $n_i = (-1)^{i+1}\left|\mathbf{S}_i\right|$, where $\left|\mathbf{S}_i\right|$ is the determinant of the 2x2 submatrix of $\mathbf{S}$ with column *i* removed. Applying this to the 3-cable CDDR yields:

$$\mathbf{N} = \begin{Bmatrix} n_1 \\ n_2 \\ n_3 \end{Bmatrix} = \begin{Bmatrix} \sin(\theta_3 - \theta_2) \\ \sin(\theta_1 - \theta_3) \\ \sin(\theta_2 - \theta_1) \end{Bmatrix} \tag{12}$$

Now, the allowable cable angle ranges are $0 \le \theta_1 \le 60^\circ$, $120^\circ \le \theta_2 \le 180^\circ$, and $240^\circ \le \theta_3 \le 300^\circ$. Therefore, the three possible delta angle ranges in (12) are $60^\circ \le \theta_3 - \theta_2 \le 180^\circ$, $-300^\circ \le \theta_1 - \theta_3 \le -180^\circ$, and $60^\circ \le \theta_2 - \theta_1 \le 180^\circ$. Note all three ranges are identical since the second condition is identical to

$60^\circ \le \theta_1 - \theta_3 \le 180^\circ$. The *sine* of all these delta angles is always positive as long as $60^\circ \le \theta_j - \theta_k < 180^\circ$ (the *sine* is zero when any delta angle is equal to $180^\circ$). Therefore, *the entire allowable kinematic workspace of the base triangle is also the statics workspace*! So, there is no limitation due to considering only positive cable tensions! On the edge of the base triangle one $n_i = 0$ and thus the triangle edges are not in the statics workspace. Recall from the forward velocity solution presented in Section 3.2, the triangle edges also correspond to kinematic singularities. At all points outside of the base triangle, 2 components of the kernel vector **N** have the same sign and the other component has the opposite sign so outside the base triangle is also outside of the statics workspace.

For on-line control of a planar CDDR with one degree of actuation redundancy, the cable tensions for control are calculated by (11) and (12), choosing $\alpha$ so that one component of **T** is zero (or, a small positive value) and the remaining terms are positive.

***4.2.2 Two Degrees of Actuation Redundancy.*** For CDDRs with two or more degrees of actuation redundancy (the planar 4-cable case in this paper), determination of the statics workspace and the method for maintaining positive cable tensions are more complicated. For actuation redundancy of degree two, an equivalent expression for (10) is:

$$\mathbf{T} = \begin{Bmatrix} t_{P1} \\ t_{P2} \\ t_{P3} \\ t_{P4} \end{Bmatrix} + \alpha \begin{Bmatrix} n_1 \\ n_2 \\ n_3 \\ n_4 \end{Bmatrix} + \beta \begin{Bmatrix} m_1 \\ m_2 \\ m_3 \\ m_4 \end{Bmatrix} \tag{13}$$

where the particular solution $\mathbf{S}^+\mathbf{F}_R$ is again the first term in (13) and the homogeneous solution is expressed as the two kernel vectors of **S** ($\mathbf{N} = \{n_1 \quad n_2 \quad n_3 \quad n_4\}^T$ and $\mathbf{M} = \{m_1 \quad m_2 \quad m_3 \quad m_4\}^T$) multiplied by arbitrary scalars $\alpha$ and $\beta$. Given (13), the condition for a CDDR configuration to lie within the statics workspace is:

$$\alpha \begin{Bmatrix} n_1 \\ n_2 \\ n_3 \\ n_4 \end{Bmatrix} + \beta \begin{Bmatrix} m_1 \\ m_2 \\ m_3 \\ m_4 \end{Bmatrix} > \begin{Bmatrix} 0 \\ 0 \\ 0 \\ 0 \end{Bmatrix} \tag{14}$$

Divide the workspace into four sectors as in Fig. 4. We can construct a different null space basis for each sector. This is required to demonstrate that the entire workspace is within the statics workspace.

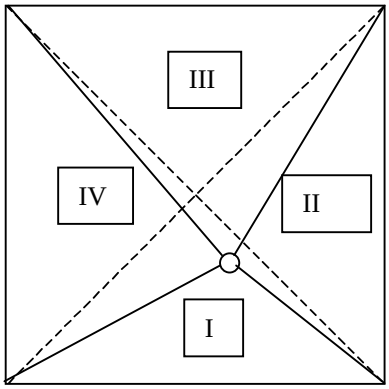


*Figure 4. Planar 4-Cable CDDR Workspace Sectors*

*Case I*: Let us suppose that the end-effector point is in the first sector. A possible basis for the null space is:

$$\mathbf{N} = \begin{Bmatrix} \sin(\theta_4 - \theta_2) / \sin(\theta_2 - \theta_1) \\ \sin(\theta_1 - \theta_4) / \sin(\theta_2 - \theta_1) \\ 0 \\ 1 \end{Bmatrix} \quad \mathbf{M} = \begin{Bmatrix} \sin(\theta_3 - \theta_2) / \sin(\theta_2 - \theta_1) \\ \sin(\theta_1 - \theta_3) / \sin(\theta_2 - \theta_1) \\ 1 \\ 0 \end{Bmatrix} \tag{15}$$

If the end-effector lies within sector I, the allowable cable angle ranges are $0^\circ < \theta_1 \le 45^\circ$, $135^\circ < \theta_2 \le 180^\circ$, $225^\circ \le \theta_3 < 270^\circ$, and $270^\circ < \theta_4 < 315^\circ$. Note that the sector triangle edges are included. The possible delta angle ranges are $90^\circ < \theta_4 - \theta_2 < 135^\circ$, $90^\circ < \theta_2 - \theta_1 < 180^\circ$, $-270^\circ < \theta_1 - \theta_3 \le -180^\circ$, $-315^\circ < \theta_1 - \theta_4 < -225^\circ$, and $45^\circ < \theta_3 - \theta_2 < 135^\circ$. Therefore all the sine functions in (15) are positive or null and any combination of **N** and **M** (with positive coefficients $\alpha$ and $\beta$) always has positive components as required in (14). In conclusion, the first sector belongs to the statics workspace.

*Case II*: Let us suppose that the end-effector point is in the second sector. We can choose a different basis for the null space:

$$\mathbf{N} = \begin{Bmatrix} 0 \\ \sin(\theta_4 - \theta_3) / \sin(\theta_3 - \theta_2) \\ \sin(\theta_2 - \theta_4) / \sin(\theta_3 - \theta_2) \\ 1 \end{Bmatrix} \quad \mathbf{M} = \begin{Bmatrix} 1 \\ \sin(\theta_1 - \theta_3) / \sin(\theta_3 - \theta_2) \\ \sin(\theta_2 - \theta_1) / \sin(\theta_3 - \theta_2) \\ 0 \end{Bmatrix} \tag{16}$$

If the end-effector lies within sector II, the allowable cable angle ranges are $0^\circ < \theta_1 \le 45^\circ$, $90^\circ < \theta_2 \le 135^\circ$, $225^\circ < \theta_3 < 270^\circ$, and $315^\circ \le \theta_4 < 360^\circ$. The possible delta angle ranges are $45^\circ < \theta_4 - \theta_3 < 135^\circ$, $-225^\circ < \theta_2 - \theta_4 \le -180^\circ$, $-270^\circ < \theta_1 - \theta_3 < -180^\circ$, $45^\circ < \theta_2 - \theta_1 < 135^\circ$, and $90^\circ < \theta_3 - \theta_2 < 180^\circ$. Therefore all the sine functions in (16) are positive or null and any combination of **N** and **M** (with positive coefficients $\alpha$ and $\beta$) always has positive components. In conclusion, the second sector also belongs to the statics workspace.

The last two cases are similar. Choose:

$$\mathbf{N} = \begin{Bmatrix} 0 \\ 1 \\ \sin(\theta_2 - \theta_4) / \sin(\theta_4 - \theta_3) \\ \sin(\theta_3 - \theta_2) / \sin(\theta_4 - \theta_3) \end{Bmatrix} \quad \mathbf{M} = \begin{Bmatrix} 1 \\ 0 \\ \sin(\theta_1 - \theta_4) / \sin(\theta_4 - \theta_3) \\ \sin(\theta_3 - \theta_1) / \sin(\theta_4 - \theta_3) \end{Bmatrix} \tag{17}$$

as a suitable basis for sector III and:

$$\mathbf{N} = \begin{Bmatrix} \sin(\theta_3 - \theta_4) / \sin(\theta_4 - \theta_1) \\ 0 \\ 1 \\ \sin(\theta_1 - \theta_3) / \sin(\theta_4 - \theta_1) \end{Bmatrix} \quad \mathbf{M} = \begin{Bmatrix} \sin(\theta_2 - \theta_4) / \sin(\theta_4 - \theta_1) \\ 1 \\ 0 \\ \sin(\theta_1 - \theta_2) / \sin(\theta_4 - \theta_1) \end{Bmatrix} \tag{18}$$

as a suitable basis for sector IV. The conclusion for each case is identical, i.e. the third and fourth sectors also belong to the statics workspace, including all internal triangle edges. The only point we did not take into account is the center of the square, but in this case the basis of the null space is made up by only one vector $\mathbf{N} = \{1 \quad 1 \quad 1 \quad 1\}^T$ because the rank of **S** degenerates to one. Clearly this special case is within the statics workspace since it easily satisfies (14).

Therefore, we have shown that *the entire allowable kinematic workspace of the base square is also the statics workspace*! The edge of the base square (which correspond to kinematic singularities) and all points outside of the base square are outside of the statics workspace. This result makes sense given the 3-cable results since the addition of another cable can only help the statics workspace.

In the future we intend to develop a general method for on-line control of a planar CDDR with two degrees of actuation redundancy (i.e. find optimal $\alpha$ and $\beta$ for (13)). In this paper we take a simple approach: given the current CDDR configuration and the commanded Cartesian force $\mathbf{F}_R$, we determine which two cables align most nearly with the Cartesian force direction. Then we set the remaining two cables tensions to zero (or, small positive values) and calculate the two active cable tensions with a reduced, square 2x2 system of equations from (9b). Proper choice of the active cables can always result in strictly positive cable tensions. In the examples of the following section, two cables were always set to zero tension for the 4-cable CDDR (the choice of which cables are active changes with configuration and $\mathbf{F}_R$); in practice these tensions should be set to small positive values and accounted for by bringing the known portion to the right-hand-side of (9b) while constructing the reduced square 2x2 system of equations.

## 5. EXAMPLES

This section presents position kinematics and statics examples for the planar 3-cable CDDR with one degree of actuation redundancy and for the planar 4-cable CDDR with two degrees of actuation redundancy. The base polygons are regular (equilateral triangle and square as shown in Figs. 1 and 2); the triangle side is $L_B$ = 1 *m*. For a fair comparison between these CDDRs the square side length for the 4-cable case was chosen so that both base polygons encompass the same area: for the square, $L_B$ = 0.6580 *m*. Note this is different than the cases shown in Figs. 1 and 2 where both triangle and square sides $L_B$ are shown equal.

The simulated task is for the CDDR end-effector point $\mathbf{X} = \{x \quad y\}^T$ to trace a circle in the plane while exerting a given constant Cartesian force $\mathbf{F}_R$ on the environment. The identical task will be performed by both 3-cable and 4-cable CDDRs and the results will be compared. The circle is centered at the base polygon centroid (the origin of {**0**}) and the circle radius is arbitrarily chosen to be three-quarters of the shortest distance from the base triangle centroid to a triangle side: $r$ = 0.2165 *m*. Figures 5 and 6 show the simulated task to scale for the 3- and 4-cable cases, respectively, at the starting (and ending) point. We define polar angle $\phi$ as the independent parameter for the circle; it is measured using the right-hand from the right horizontal to the circle radius; $\phi$ is shown as 0 (and $360^\circ$) in Figs. 5 and 6. All results below are plotted against $\phi$.

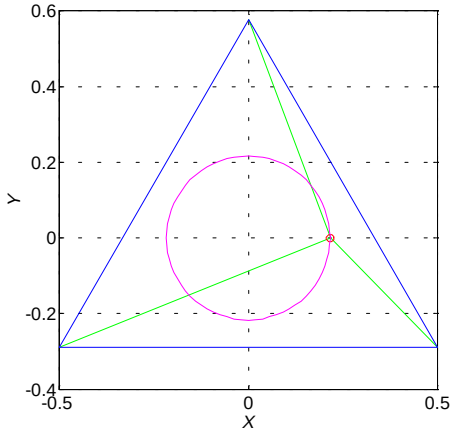


*Figure 5. Planar 3-Cable CDDR Example Task*

Figure 7a shows the required 3-cable CDDR lengths to complete the circle task and Fig. 7b shows the required 3-cable CDDR tensions to exert a constant Cartesian force of $\mathbf{F}_R = \{0 \quad 1\}^T$ *N*. To compare, Fig. 8a shows the required 4-cable CDDR lengths to complete the circle task and Fig. 8b shows the required 4-cable CDDR tensions to exert a constant Cartesian force of $\mathbf{F}_R = \{0 \quad 1\}^T$ *N*.

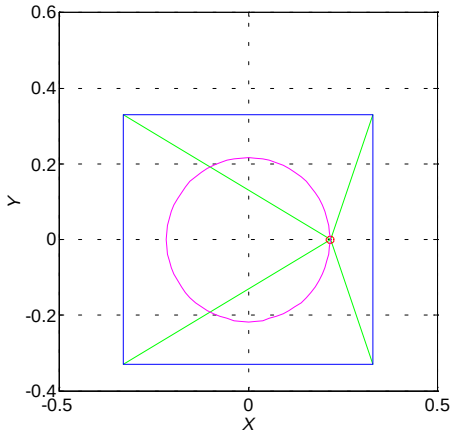


*Figure 6. Planar 4-Cable CDDR Example Task*

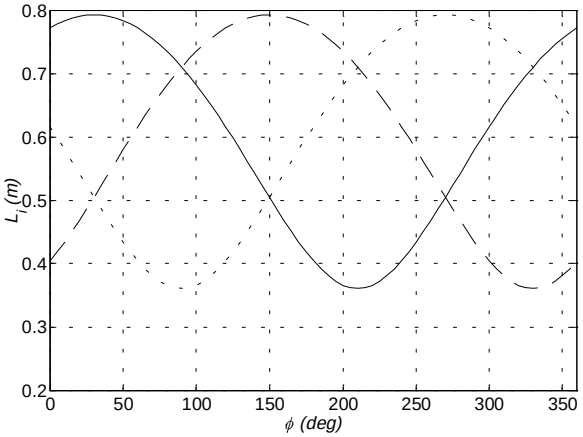


*Figure 7a.* $L_1$ (solid), $L_2$ (long dash), $L_3$ (short dash) *for Circle*

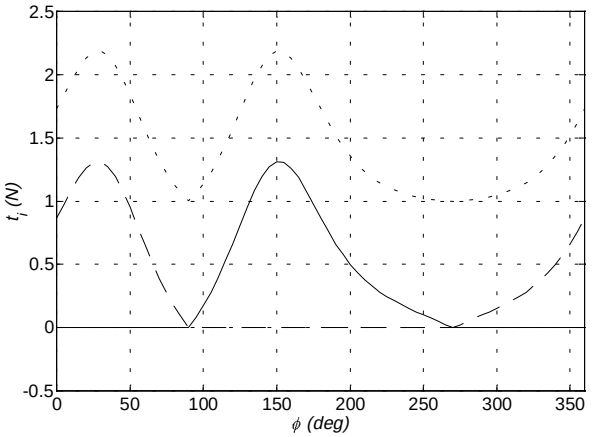


*Figure 7b.* $t_1$ (solid), $t_2$ (long dash), $t_3$ (short dash) *for* $\mathbf{F}_R = \{0 \quad 1\}^T$

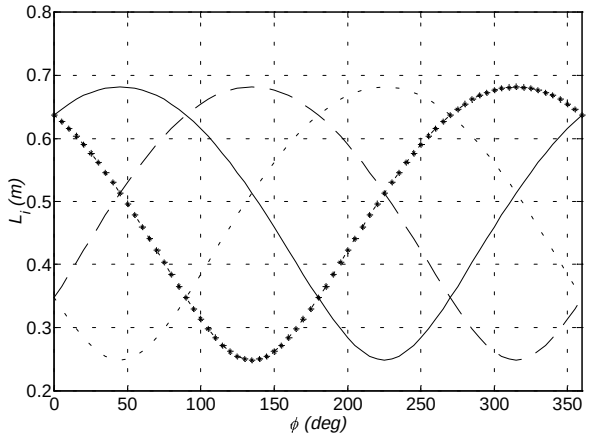


*Figure 8a.* $L_1$ (solid), $L_2$ (long dash), $L_3$ (short dash), $L_4$ (asterisk) *for Circle*

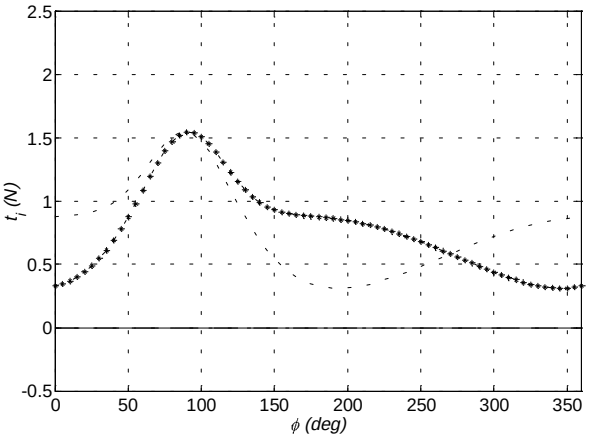


*Figure 8b.* $t_1$ (zero), $t_2$ (zero), $t_3$ (short dash), $t_4$ (asterisk) *for* $\mathbf{F}_R = \{0 \quad 1\}^T$

Comparing Figs. 7a and 8a, it is seen that the cable lengths are cyclical functions for the circle task when plotted against $\phi$. Each has its own special symmetry, but the 4-cable lengths are generally shorter than those required for the 3-cable CDDR. Comparing Figs. 7b and 8b, it is seen that the cable tensions are generally lower for the 4-cable case than for the 3-cable case. For the 3-cable CDDR of Fig. 7b, the zero-tension cable alternates between cables 1 and 2 (Figs. 1 and 2 give the cable numbering for the 3- and 4-cable cases, respectively), switching at $\phi = 90^\circ$ and $\phi = 270^\circ$. For the 4-cable CDDR of Fig. 8b, the zero-tension cables are always cables 1 and 2 due to the given constant Cartesian force $\mathbf{F}_R = \{0 \quad 1\}^T$.

To compare the 3- and 4-cable CDDRs in the same task with different constant Cartesian forces, Figs. 9a, 9b, and 9c compare the norms of cable tensions for the two CDDRs, for Cartesian forces $\mathbf{F}_R = \{0 \quad 1\}^T$, $\mathbf{F}_R = \{0.707 \quad 0.707\}^T$, and $\mathbf{F}_R = \{1 \quad 0\}^T$, respectively. In this paper we use the one-norm definition: $\|\mathbf{T}\|_1 = \sum_{i=1}^{n} |t_i|$, where the absolute value of each tension component is summed and $n$=3 or 4 for the 3- and 4-cable CDDRs, respectively. Note that, despite the fact that the norms involve 3 tensions in the first CDDR and 4 tensions in the second, the required tensions are lower for the 4-cable CDDR than the 3-cable CDDR. This tension norm measure is proportional to the required energy, so the 4-cable CDDR is more energy-efficient in performing the same task than the 3-cable CDDR. Of course, the tradeoff is the addition of an extra actuator, with its additional hardware and decreased reliability.

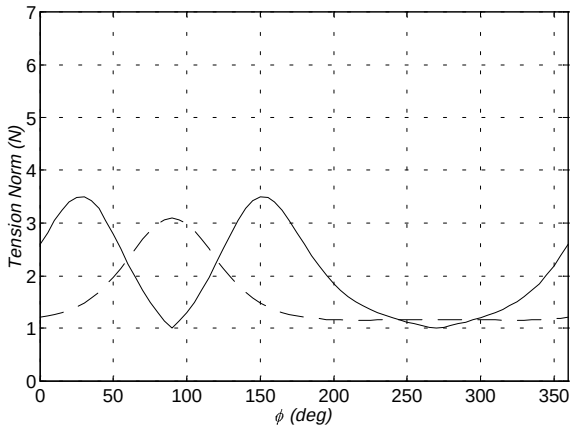


*Figure 9a. Tension Norm Comparison for the 3- (solid) and 4-cable (long dash) CDDRs for* $\mathbf{F}_R = \{0 \quad 1\}^T$

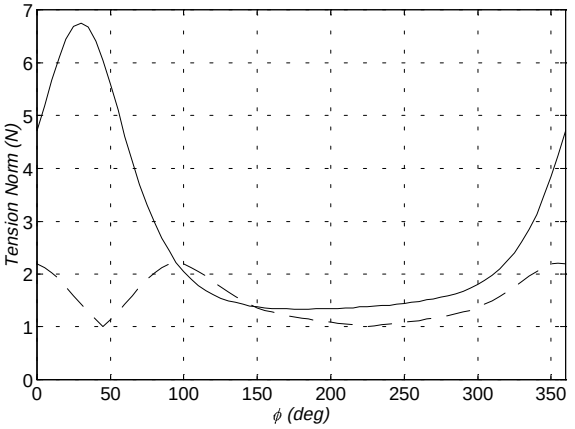


*Figure 9b. Tension Norm Comparison for the 3- (solid) and 4-cable (long dash) CDDRs for* $\mathbf{F}_R = \{0.707 \quad 0.707\}^T$

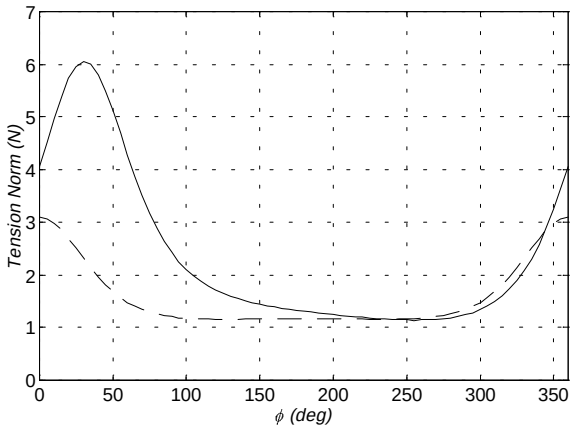


*Figure 9c. Tension Norm Comparison for the 3- (solid) and 4-cable (long dash) CDDRs for* $\mathbf{F}_R = \{1 \quad 0\}^T$

## 6. CONCLUSION

This paper introduces the concept of hybrid parallel/serial manipulators where the translational freedoms are guided by an in-parallel-over-actuated cable-direct-driven robot (CDDR) and the rotational freedoms are provided by a serial wrist mechanism. The motivation behind this work is to improve the serious cable interference and negative cable tensions possible with existing CDDRs that guide both translational and rotational freedoms. Only the translational portion is considered in this paper; kinematics and statics modeling is presented, followed by determination of the statics workspace (the space wherein all possible Cartesian forces may be exerted with only positive cable tensions), along with an example comparing the planar 3- and 4-cable cases in the same task. It was found that the 4-cable case was more energy-efficient than the 3-cable case in performing the same task. The cost is a potentially more complex cable tension algorithm (a simple approach is used in this paper) and the overhead and reduced reliability of an extra actuator.

Our future work plans include stiffness modeling, dynamics modeling (our early results are presented in a companion paper, Gallina and Williams, 2001) and controller development, hardware implementation, and experimental validation of our results.

## REFERENCES


J.S. Albus, R. Bostelman, and N.G. Dagalakis, 1993, "*The NIST ROBOCRANE*", Journal of Robotic Systems, 10(5): 709-724.

P.D. Campbell, P.L. Swaim, and C.J. Thompson, 1995, "*Charlotte Robot Technology for Space and Terrestrial Applications*", 25th International Conference on Environmental Systems, San Diego, SAE Article 951520.

C.M. Gosselin, 1996, "Parallel Computation Algorithms for the Kinematics and Dynamics of Planar and Spatial Parallel Manipulators", *Journal of Dynamic Systems, Measurement, and Control*, 118(1): 22-28.

M. Ishii and M. Sato, 1994, "*A 3D Spatial Interface Device Using Tensed Strings*", Presence-Teleoperators and Virtual Environments, MIT Press, Cambridge, MA, 3(1): 81-86.

S. Kawamura and K. Ito, 1993, "*New Type of Master Robot for Teleoperation Using a Radial Wire Drive System*", Proceedings of the IEEE/RSJ International Conference on Intelligent Robots and Systems, Yokohama, Japan, July 26-30, 55-60.

R. Lindemann and D. Tesar, 1989, "*Construction and Demonstration of a 9-String 6-DOF Force Reflecting Joystick for Telerobotics*", NASA International Conference on Space Telerobotics, (4): 55-63.

R.G. Roberts, T. Graham, and T. Lippitt, 1998, "*On the Inverse Kinematics, Statics, and Fault Tolerance of Cable-Suspended Robots*", Journal of Robotic Systems, 15(10): 581-597.

Y. Shen, H. Osumi, and T. Arai, 1994, "*Manipulability Measures for Multi-wire Driven Parallel Mechanisms*", IEEE International Conference on Industrial Technology, 550-554.

M. Sklar and D. Tesar, 1988, "*Dynamic Analysis of Hybrid Serial Manipulator Systems Containing Parallel Modules*", Journal of Mechanisms, Transmissions, and Automation in Design, 110(2): 109-115.

L.W. Tsai, 1999, Robot Analysis: The Mechanics of Serial and Parallel Manipulators, Wiley, New York.

R.L. Williams II, 1998, *"Cable-Suspended Haptic Interface"*, International Journal of Virtual Reality, 3(3): 13-21.

R.L. Williams II and P. Gallina, 2000, *"Cable-Direct-Driven Haptic Interface Design"*, submitted to the ASME Journal of Mechanical Design.

P. Gallina, A. Rossi, and R.L. Williams II, 2001, *"Planar Cable-Direct-Driven Robots, Part II: Dynamics and Control"*, submitted to the 2001 ASME Design Technical Conferences, September 9-12, Pittsburgh, PA.